Biochimica et Biophysica Acta 1850 (2015) 1253–1260

Contents lists available at ScienceDirect

Biochimica et Biophysica Acta

journal homepage: www.elsevier.com/locate/bbagen

Rhodamine B-conjugated encrypted vipericidin nonapeptide is a potent toxin to zebrafish and associated with *in vitro* cytotoxicity

Liang Wang [a], Judy Y.W. Chan [a], Juciane V. Rêgo [b,c], Cheong-Meng Chong [a], Nana Ai [a], Cláudio B. Falcão [c], Gandhi Rádis-Baptista [c,*], Simon M.Y. Lee [a,**]

[a] State Key Laboratory of Quality Research in Chinese Medicine and Institute of Chinese Medical Sciences, University of Macau, Macao, China
[b] Northeast Biotechnology Network (RENORBIO), Post-graduation program in Biotechnology, Federal University of Ceara, Brazil
[c] Laboratory of Biochemistry and Biotechnology, Institute for Marine Sciences, Federal University of Ceara, Brazil

ARTICLE INFO

Article history:
Received 24 November 2014
Received in revised form 15 February 2015
Accepted 20 February 2015
Available online 27 February 2015

Keywords:
Vipericidins
Encrypted peptides
Cell-penetrating peptide
Cytotoxin
Zebra-fish model
Rhodamine B-conjugated peptide

ABSTRACT

Background: Animal venoms contain a diverse array of proteins and enzymes that are toxic toward various physiological systems. However, there are also some practical medicinal uses for these toxins including use as anti-bacterial and anti-tumor agents.
Methods: In this study, we identified a nine-residue cryptic oligopeptide, KRFKKFFKK (EVP50) that is repeatedly encoded in tandem within vipericidin sequences.
Results: EVP50 displayed *in vivo* potent lethal toxicity to zebrafish larvae (LD_{50} = 6 μM) when the peptide's N-terminus was chemically conjugated to rhodamine B (RhoB). *In vitro*, RhoB-conjugated EVP50 (RhoB-EVP50) exhibited a concentration-dependent cytotoxic effect toward MCF-7 and MDA-MB-231 breast cancer cells. In MCF-7 cells, the RhoB-EVP50 nonapeptide accumulated inside the cells within minutes. In the cytoplasm, the RhoB-EVP50 induced extracellular calcium influx and intracellular calcium release. Membrane budding was also observed after incubation with micromolar concentrations of the fluorescent EVP50 conjugate.
Conclusions: The conjugate's interference with calcium homeostasis, its intracellular accumulation and its induced membrane dysfunction (budding and vacuolization) seem to act in concert to disrupt the cell circuitry. Contrastively, unconjugated EVP50 peptide did not display neither toxic nor cytotoxic activities in our *in vivo* and *in vitro* models.
General significance: The synergic mechanism of toxicity was restricted to the structurally modified encrypted vipericidin nonapeptide.

1. Introduction

Vipericidins (crotalicidin, batroxicidin, lutzicidin, and lachesicidin) together with Bf-CRAMP, Na-CRAMP and Oh-CRAMP comprise the cathelicidin-related antimicrobial peptides (CRAMPs) from the venom gland of the pit vipers and elapid snakes, respectively [1–3]. The cathelicidin family of peptides encompasses hundreds of sequences expressed in the tissues and cells of the immune systems of several species of vertebrates. Vipericidins and elapid CRAMPs are structurally arranged as prepropeptides with a signal peptide of ~20 residues, a conserved cathelin domain (cathepsin L inhibitor protein) and a hypervariable carboxyl-terminal stretch where a range of natural antimicrobial activities are found. Mature vipericidins and elapid CRAMPs share a high level of amino acid similarity, with most of their 34 residues being identical or strictly conserved substitutions. Due to the high proportion of lysine residues alternating with hydrophobic amino acid residues, these peptides have a net positive charge and have an amphipathic character, as observed in other membrane-active venom peptides, like anoplin [4] and mastoparans [5]. One distinctive structural feature in snake venom CRAMPs when compared to other familial members of cathelicidins is the presence of an extra acidic patch (or acidic signature) at the C-terminal end of the prosequence, which is rich in aspartic acid and uncharged residues (Fig. 1). Snake venom CRAMPs (vipericidins and elapid cathelicidins) possess effective broad-spectrum activity against clinical isolates and standard strains of bacteria and yeast [1–3,6,7]. They are particularly active against Gram-negative bacteria, even rivaling organic antimicrobial compounds. Interestingly, the cathelicidin of *Bungarus fasciatus* (BF-30) was shown to annihilate *in vitro* melanoma B16F10 cells in a dose- and time-dependent

Abbreviations: EVP, encrypted vipericidin peptide; RhoB, rhodamine B; CRAMP, cathelicidin-related antimicrobial peptide; dpf, days post-fertilization; ACP, acidic connecting peptide

* Correspondence to: G. Rádis-Baptista, Laboratory of Biochemistry and Biotechnoloy, Institute for Marine Sciences, Federal University of Ceará, Av. Da Abolição, 3207, 60165 081 Fortaleza, CE, Brazil. Tel.: +55 85 3366 7007; fax: +55 85 3366 7002.
** Correspondence to: S.M.Y. Lee, Institute of Chinese Medical Sciences, University of Macau. Av. da Universidade, Room No N22-7003. N22 Building. Taipa, Macau. Tel./fax: +853 8822 4695.
E-mail addresses: gandhi.radis@ufc.br (G. Rádis-Baptista), simonlee@umac.mo (S.M.Y. Lee).

http://dx.doi.org/10.1016/j.bbagen.2015.02.013
0304-4165/

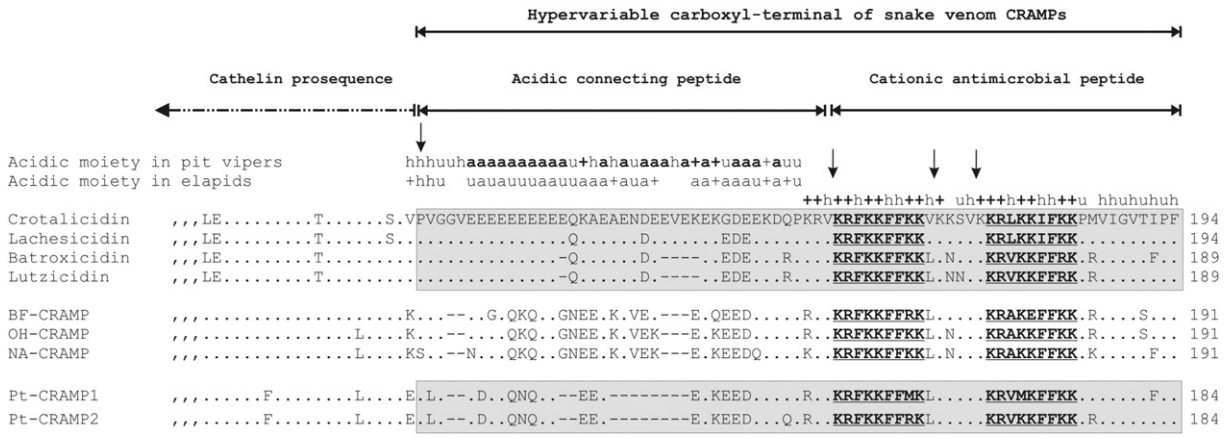

Fig. 1. Hypervariable C-terminal region of the snake venom CRAMPs and putative proteolytic cleavage sites. The acidic and cationic/amphiphatic domains of vipericidins and elapid CRAMPs were aligned. Identical amino acid residues are represented by dots, and gaps are represented by hyphens. The hypervariable anionic linkage sequences followed by the cationic antimicrobial peptides are preceded by the highly conserved cathelin prosequence (indicated by a slash). The *in tandem* repetitive cryptic nonapeptides embedded in the mature antimicrobial sequences are in bold and underlined. Arrows indicate putative proteolytic cleavage sites. The "a", "h" and "u" lowercase letters and the "+" symbol represent acidic, hydrophobic, uncharged and basic amino acid residues, respectively. Numbers on the right side of each polypeptide sequence refer to the number of residues that a given cathelicidin-related pre-propeptide contains. The vipericidins (crotalicidin, lachesicidin, batroxicidin and lutzicidin) and *P. textilis* CRAMPs (PT-CRAMP1 and 2) C-termini are shown in gray.

fashion and inhibit melanoma growth and metastasis in grafted mice [8]. On the same spectrum of activity, a Lys-16 mutant of BF-30 (BF30-K16) displayed selective *in vitro* cytotoxicity against lung cancer cell propagation in a concentration range that was not toxic to non-tumor cell lines [9].

Pre-propeptides, like the cathelicidin precursors, are processed by specific proteases that release the active portion of the polypeptide responsible for a given biological effect. Animal toxin peptides are also processed into their mature active form by precise proteolysis. For instance, crotamine and crotamine-like peptides from snake venom and lizards [10,11], cytolysins from sea anemones [12,13], apamin, melittin and mastoparan-B from hymenoptera venom [14,15], conotoxins from the marine gastropods *Conus* [16,17] and antimicrobial and cytolytic peptides from spider venom [18] are all toxins that mature by proteolytic cleavage. A less obvious maturation process (post-translational modification) is the proteolytic release of a number of bioactive peptides that are encrypted within longer polypeptides. Classic examples of cryptic peptides that contain natural physiologically active human cryptomes include the proteolytically activated prohormone precursor pro-opiomelanocortin (POMC) and the extracellular-matrix-derived crypteins [19]. In the first example, dozens of diverse active hidden opioid peptides with distinct pharmacological functions are released from POMC by tissue-specific convertases (proteases). In the second example, encrypted peptides with anti-angiogenic, anti-tumor, immunomodulation, antimicrobial and chemotaxis activities are proteolytically cleaved from proteins in the extracellular matrix, such as collagens, laminin and perlecan [19]. Thus, biological systems utilize proteolytic cleavage to generate encrypted peptides and to increase the structural, molecular and pharmacological diversity of a given peptidome to elicit complex physiological and pathophysiological responses in mammals.

Snake venom cathelicidins contain several proteolytic cleavage sites that can potentially produce a diverse array of smaller peptides [1,2]. It was proposed that elastase-like proteases are involved in the processing of bovine and porcine cathelicidins and potentially fowlicidins — cathelicidins from chicken [20]. Thus, it was anticipated that vipericidins and elapid CRAMPs might give rise to several hidden bioactive peptides from the lysine-rich, α-helical, carboxyl-terminal antimicrobial sequences. We focused our attention on the C-terminal hypervariable region of vipericidins and prepared synthetic peptides conjugated to rhodamine-B. The toxic and cytotoxic activities of encrypted vipericidin peptides were evaluated *in vivo* with zebrafish model of vertebrate organism and *in vitro* with two lines of human breast cancer cells, MCF-7 and MDA-MB231. The cell uptake and intracellular accumulation, the membrane disturbance and the interference with calcium homeostasis were observed for a criptic vipericidn nonapeptide (KRFKKFFKK) that was covalently linked to rhodamine B.

2. Materials and methods

2.1. Peptide sequences and synthesis

The hypervariable C-terminus of the vipericidins, which served as template sequences for synthesis of the encrypted peptides, was from lachesicidin (GenBank accession number AGS36142.1), which shares a high degree of sequence identity with crotalicidin (99%, AGS36138.1), batroxicidin (85%, AGS36140.1), lutzicidin (84%, AGS36141.1), Bf-CRAMP (65%, B6D434), Oh-CRAMP (65%, B6S2X2.1), and Na-CRAMP (64%, B6S2X0.1). Batroxicidin was also used for the design and synthesis of an acidic cryptic peptide (Fig. 1). All peptides were synthesized by solid phase chemistry and obtained at a purity grade over 95% and confirmed by the presence of a single peak in analytical reverse-phase HPLC and mass spectrometry analysis (Cellmano Biotech Limited, Hefei, China). The fluorescent dye Rhodamine B was covalently linked to the N-terminal end of the peptide series, directly to N-deblocked chain of peptide attached to the resin. Complete deprotection and cleavage was carried out essentially with trifluoroacetic acid in water. The crude peptides were precipitated out by the addition of chilled ether. Then, the crude peptide was purified by HPLC, freeze-drying and re-tested by HPLC to make sure that it is qualified. Table 1 summarizes the synthetic encrypted vipericidin peptides used in this study.

2.2. Zebrafish maintenance

The enhanced green fluorescent protein (EGFP) was specifically expressed in the endothelial cells of *Tg*(*fli-1:EGFP*) zebrafish larvae. The zebrafish used in our study were maintained as previously described [21]. Natural pair-wise mating (3–12 months old) was used to generate zebrafish embryos. The embryos were raised and maintained in "embryo medium" at 28.5 °C. Ethic approval for the animal experiments was granted by the Animal Research Ethics Committee in University of Macau, University of Macau, China.

2.3. Acute toxicity of encrypted vipericidin peptides toward zebrafish

Zebrafish larvae at three days post-fertilization (3dpf) were separated into a 24-well plate and exposed to 2-logs (from 1 to 100 μM)

Table 1
Primary structures, molecular weights, physicochemical characteristics and toxicity levels of rhodamine B-conjugated peptides derived from vipericidin hypervariable C-terminal regions.

Peptides[a]	Primary sequences[b]	MW	pI[c]	Net charge[c](z)	LD_{50} (μM)[d]
ACP1b	RhoB—PVGGVEEEEEDEEEQKAEVEKDEEKEDEEKDRPKRVKRFKKFFKK	5935.5	4.52	−6	16
ACP1l	RhoB—PVGGVEEEEEEEEEEQKAEAENDEEVEKEKEDEEKDQPKRVKRFKKFFKK	6495.0	4.28	−10	13
ACP18b	RhoB—EEEEEDEEEQKAEVEKDEEKE	3035.1	3.59	−12	105
ACP18l	RhoB—EEEEEEEEEEQKAEAENDEEV	2978.0	3.13	−14	123
ACP41b	RhoB—EKDEEKEDEEKDRPKRV	2584.9	4.44	−3	116
ACP41l	RhoB—EKEKEDEEKDQPKRV	2312.6	4.56	−2	106
EVP26	RhoB—ENDEEV	1159.3	2.89	−4	>200
EVP50	RhoB—KRFKKFFKK	1682.2	11.85	+6	6

[a] ACP: acidic connecting (vipericidin) peptide; EVP—encrypted vipericidin peptide. Values of molecular weight and isoelectric point are for unlabeled peptides. Batroxicidin-derived peptides: "b"; lachesicidin-derived peptides: "l".
[b] The fluorochrome rhodamine-B (RhoB) is covalently linked to peptide N-terminal; the carboxyl-terminal is free. Data of toxicity are for rhodamine-B labeled peptides. Unlabeled peptides are innocuous.
[c] Values of pI and net charge are for unlabeled peptides. A pH-dependent extra charge (positive, at pH < 6.0; negative, at pH > 10.8) is imparted by rhodamine-B to peptide molecule. At pH between 6.0 and 10.8, rhodamine-B is neutral (uncharged) [22].
[d] LD_{50} denotes the concentration of rhodamine-B conjugated peptides that cause 50% of zebrafish death.

concentration of Rhodamine B-conjugated ACPs (RhoB-ACP1b, RhoB-ACP1l, RhoB-ACP18b, RhoB-ACP18l, RhoB-ACP41b and RhoB-ACP41l) and Rhodamine B-conjugated EVPs (RhoB-EVP26 and RhoB-EVP50) for 24 h. The acute toxicity and mortality of zebrafish exposed to the RhoB conjugates were determined by monitoring the absence of a heartbeat, as observed under a light microscope. Unconjugated peptides were concomitantly used in parallel in all experiments.

2.4. Distribution of RhoB-EVP50 in zebrafish and determination of acute toxicity

Zebrafish larvae were exposed to a fixed concentration (10 μM) of either RhoB-EVP50 or free rhodamine B for 24 h and mounted on microscope glass slides. The distribution of Rhodamine B-conjugated EVP50 in zebrafish body and tissues was visualized using an IX81 motorized inverted fluorescent microscope (Olympus Co., Tokyo, Japan).

2.5. RhoB-EVP50 cell uptake by tumor cells

Human breast cancer MCF-7 and MDA-MB23 cells were cultured in Dulbecco's Modified Eagle's Medium (DMEM) containing 10% fetal bovine serum and 100 IU ml^{-1} penicillin–streptomycin at 37 °C in a humidified incubator containing 5% CO_2. Cells were seeded into a 96-well plate at a density of 5×10^3 cells per well and incubated overnight. After 24 h of seeding, breast cancer cells were treated with 10 and 40 μM RhoB-EVP50 for 10 min or 60 min. Then, the cells were stained with Hoechst 33342 to label the nuclear DNA. Immortalized rat cardiomyocytes (H9c2 cardiomyoblasts) and human lung carcinoma A549 cells were similarly maintained and treated. The sub-cellular distribution of Rhodamine B-conjugated EVP50 was detected by an IN CELL Analyzer 2000 system (GE Healthcare Life Sciences, Piscataway NJ, USA).

2.6. Assessment of cell viability and cytotoxicity

The MCF-7 and MDA-MB-231 cells (1×10^4 per well) were cultured as above and treated with increasing concentrations (up to 40 μM) of RhoB-EVP50 for 1 h. The level of lactate dehydrogenase (LDH) in the medium was measured by using a Cytotoxicity Detection Kit (Roche Diagnostics Co., Indianapolis, USA) according to the protocol from the manufacturer. Cell viability was determined by a standard 3-(4,5-Dimethylthiazol-2-yl)-2,5-diphenyltetrazolium bromide (MTT) assay.

2.7. Measurement of intracellular calcium concentration

The MCF-7 cells were seeded on glass coverslips placed into the bottom of the wells of 12-well plate. Twenty-four hours after seeding, the cells were stained with 3 μM Fluo-3/AM for 30 min at 37 °C. The cells were then washed with phosphate-buffered saline (PBS) three times, and the calcium levels in the MCF-7 cells were detected using the Cell^R imaging system of an IX81 microscope (Olympus Co., Tokyo, Japan).

3. Results

3.1. Assessment of lethal toxicity of encrypted vipericidin peptides in zebrafish

From the snake venom CRAMPs shown in Fig. 1, peptides derived from the C-terminus of the vipericidins lachesicidin and batroxicidin were chemically synthesized by standard solid phase chemistry with rhodamine B covalently linked to the peptide N-terminus. The synthesized peptides and their physiochemical properties are listed in Table 1. In a screen of the lachesicidin and batroxicidin acidic connecting peptides (ACPs, namely ACPls and ACPbs, respectively) and encrypted vipericidins peptides (EVPs), the peptides RhoB-ACP1l, RhoB-ACP1c and RhoB-EVP50 showed the highest acute lethal toxicity to the zebrafish larvae (Table 1). RhoB-EVP50 was the most potent peptide, exhibiting an LD_{50} value <10 μM, and was selected for further studies.

3.2. Distribution of RhoB-EVP50 in zebrafish tissue

To determine whether Rhodamine B-conjugated EVP50 is able to enter zebrafish larvae, a number of zebrafish larvae (3dpf) were incubated with Rhodamine B-conjugated EVP50 (10 μM) for 24 h, and the rhodamine B accumulation and emission were recorded using fluorescence microscopy. Free rhodamine B was used as negative control. Fig. 2A and B show that free rhodamine B accumulated exclusively in the yolk of the zebrafish. In contrast, RhoB-EVP50 was distributed to the blood vessels (Fig. 2E and F) and co-localized with the green fluorescence of EGFP in *Tg*(*fli1:EGFP*) transgenic zebrafish (Fig. 2C and D). Fig. 2G and H demonstrated the distribution overlap pattern of Rhodamine B-conjugated EVP50 and EGFP expression in zebrafish. The merged images (Fig. 2G, H) showed that RhoB-EVP50 specifically accumulated in the posterior cardinal vein (Fig. 2E, F) and in the intersegmental vessels (Fig. 2F, H). RhoB-EVP50 was also detected in the H9c2 cardiomyoblast and heart of live zebrafish (Fig S1 and Video S1).

3.3. Cellular uptake of RhoB-EVP50

The distribution of RhoB-EVP50 in human breast cancel cell, in this case MCF-7 cell line, was detected in a similar manner using fluorescence microscopy. Fig. 3 showed that at 10 μM, RhoB-EVP50 entered and distributed uniformly and accumulate in MCF-7 cells. At higher concentrations (40 μM) and longer period of incubation (60 min *versus*

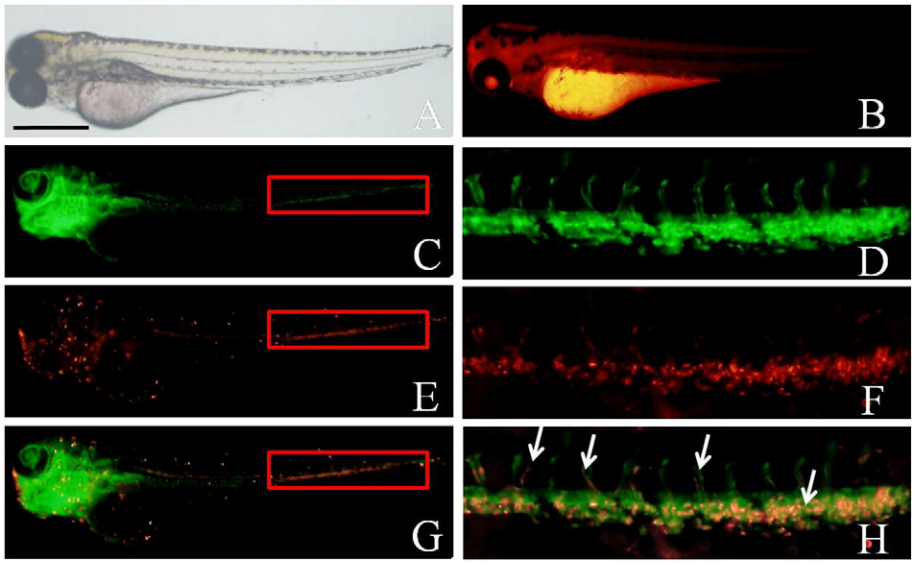

Fig. 2. Fluorescent images of the distribution of RhoB-EVP50 in *Tg(fli1: EGFP)* zebrafish. Bright field microphotography (A, B) of zebrafish (3dpf) treated with 10 μM of free rhodamine B for 24 h as a negative control. Green fluorescence pattern of EGFP expression in transgenic *Tg(fli1: EGFP)* zebrafish (C, D). Fluorescent images (E, F) from zebrafish (3dpf) after incubation with RhoB-EVP50 (10 μM) for 24 h. Merged fluorescent images (G, H) of blood vessels (green) and rhodamine-conjugated EVP50 (red). (D, F and H) Magnified images of zebrafish as shown by red box in figure C, E and G. Scale bar: 500 μm.

10 min), the dye-conjugated nonapeptide RhoB-EVP50 damaged the cell membrane and caused MCF-7 cell lyses that initiated within a 5 min time frame (Fig. 3 and Video S2). RhoB-EVP50 was also able to penetrate embryonic rat ventricle H9c2 cardiomyoblasts in culture, spread into the cytoplasm and the nucleus (Fig. S1).

3.4. Toxicity of RhoB-EVP50 toward MCF-7 and MDA-MB-231 breast tumor cells

The cell viability and cytotoxicity of RhoB-EVP50 toward MCF-7 and MDA-MB-231 cells were determined by LDH and MTT assays, respectively. As shown in Fig. 4, treatment with RhoB-EVP50 for 1 h significantly decreased the viability and increased the cytotoxicity of MCF-7 and MDA-MB-231 cells in a dose-dependent manner. As observed, in Fig. S2 unlabeled EVP50 was harmless to both tumor cell lines.

3.5. Rhodamine B-conjugated EVP50 promoted changes in intracellular calcium

The dynamics of intracellular calcium levels were measured after incubating MCF-7 cells in a fixed concentration of RhoB-EVP50. Fig. 5A

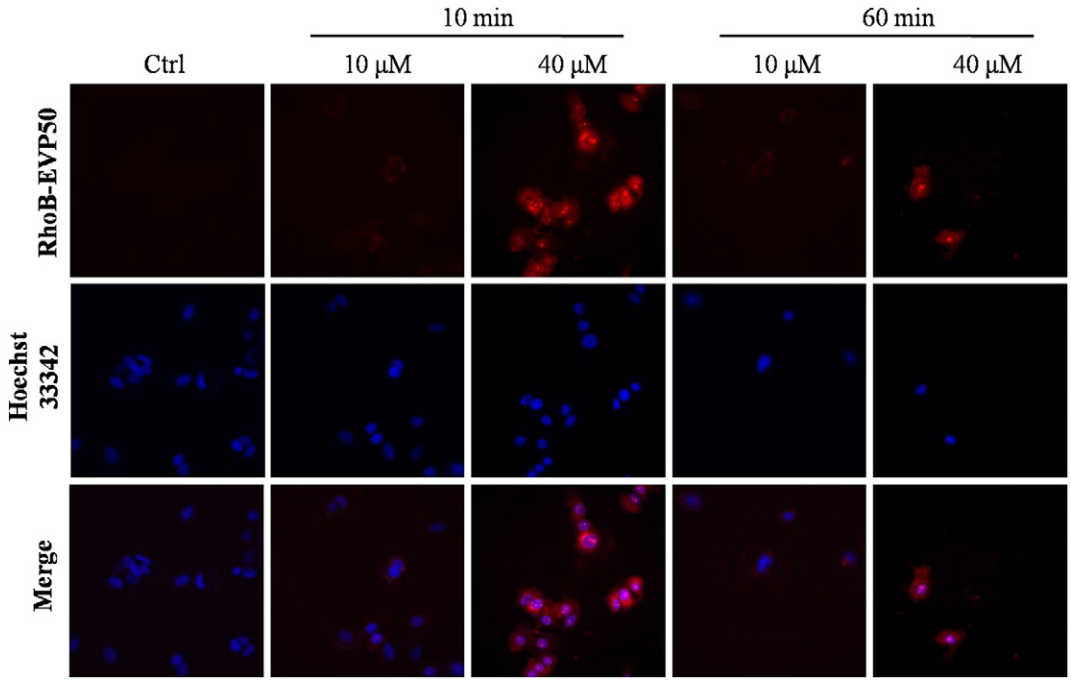

Fig. 3. Fluorescent images of the intracellular distribution of rhodamine B-conjugated EVP50 in MCF-7 cells. MCF-7 cells were treated with different concentrations of encrypted vipericidin RhoB-conjugated nonapeptide EVP50 for 10 min and 60 min. At higher concentrations (40 μM), RhoB-EVP50 is distributed in the cytoplasm and accumulated in different organelles of MCF-7 cells. Furthermore, it was showed in Supplementary data that treatment with a high concentration (40 μM) of RhoB-EVP50 for 60 min incubation, the dye-conjugated nonapeptide damaged the cell membrane and caused lyses of MCF-7 cells that initiated within a 5 min time frame.

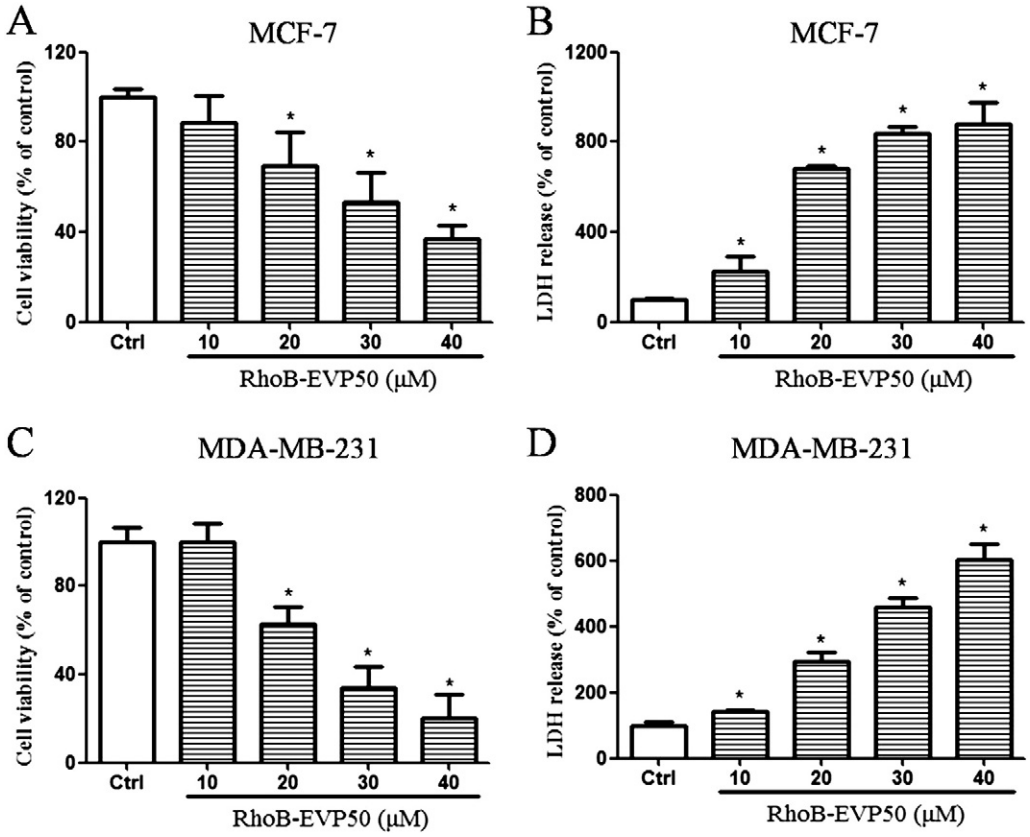

Fig. 4. Rhodamine B-conjugated EVP50 induces cell death in MCF-7 and MDA-MB-231 cells. The cells were treated with different concentrations of RhoB-EVP50 for 1 h. Cell viability and membrane integrity were evaluated by an MTT cytotoxic assay (A, C) and an LDH leakage assay (B, D), respectively. $^{*}P < 0.05$ *vs.* untreated control (Ctrl).

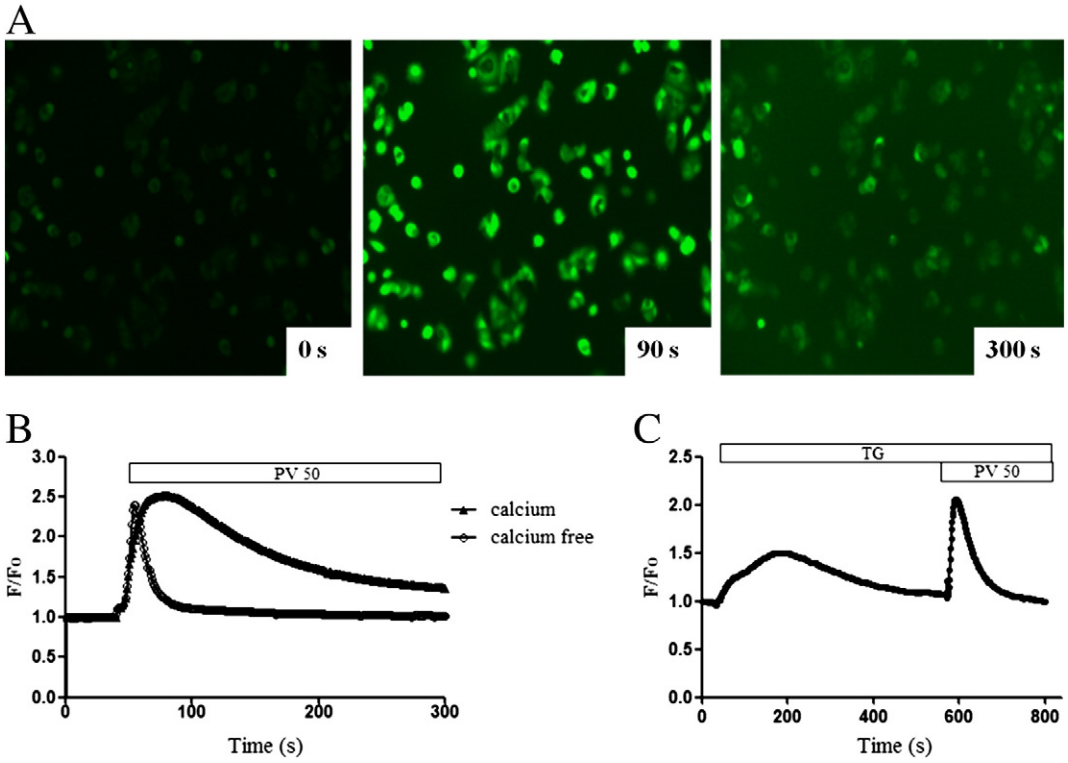

Fig. 5. Rhodamine B-conjugated EVP50 induces calcium influx and intracellular calcium release in MCF-7 cells. (A) Representative images of $[Ca^{2+}]_i$ intensity in MCF-7 cells before and after treatment with RhoB-EVP50 (30 μM). (B) RhoB-EVP50 caused $[Ca^{2+}]_i$ elevation in the absence or presence of extracellular calcium. F/F_0 represents the fluorescence signal relative to the baseline fluorescence intensity. (C) Effect of RhoB-EVP50 on $[Ca^{2+}]_i$ after intracellular calcium store depletion caused by thapsigargin (TG).

shows that RhoB-EVP50 treatment for 90 s caused a rise in the intracellular calcium fluorescence intensity when compared to the control group. Treatment of MCF-7 cells with RhoB-EVP50 for 5 min compromised the cell membrane and caused the release of the cytoplasm from cells, as evidenced by an increased fluorescent background when compared to the control group. The dynamic change in intracellular calcium levels mediated by RhoB-EVP50 in the treated MCF-7 cells was also recorded (Video S2). As shown in Fig. 5B, the levels of cytosolic calcium increased after the addition of RhoB-EVP50 in the presence or absence of extracellular calcium, which indicated that RhoB-EVP50 caused extracellular calcium influx and intracellular calcium release from the endoplasmic reticulum into the cytosol in MCF-7 cells. This is consistent with the data presented in Fig. 5C, which show that RhoB-EVP50 also induced an increase in calcium levels even if calcium stores were depleted with thapsigargin (TG) — an endoplasmic reticulum Ca^{2+}-ATPase inhibitor.

4. Discussion

Cathelicidins are broad-spectrum antimicrobial peptides and multifunctional host-defense effectors of innate immune system of vertebrates, which are phylogenitically as distant as the extant fossil fish (hagfish) and the humans [23,24]. Recently, four new snake venom cathelicidin-related antimicrobial peptide (svCRAMP) sequences were identified from South American pit vipers (rattlesnakes and jararacas), that collectively were named vipericidins, and two novel elapid CRAMPs from *Pseudonaja textilis*. [1]. These svCRAMPs are potent bactericides and display an efficacious anticancer activity due to their ability to disrupt the biological membranes, interact to nucleic acids, and rapidly kill microbial and tumor cells [1,3,6–9]. Whether vipericidins and elapid CRAMPs have a primary antimicrobial role in protecting the venom glands from microbial infection or if they contribute with other venom components to intensify the tissue damage caused by snake envenomation deserves further investigation. The vipericidins and elapid CRAMP prepropeptides, like other members of cathelicidin family, are converted into the mature form by post-translational proteolytic processing, which then releases the α-helical antimicrobial peptides that are located in the variable carboxyl-terminal of prosequences [1,2,20,25]. Analysis of the complete amino acid sequences of vipericidins reveals several putative protease cleavage sites, such as the dipeptides KK, KR and VK (Fig. 1). Therefore, diverse encrypted peptides can be formed after post-translational proteolytic modification of longer polypeptide precursors [26,27], releasing cryptic peptide sequences whose biological functions and potential toxicities are unpredictable and must be experimentally ascertained. Additionally, propeptide sequences with unknown biological activity in certain classes of proteins can be proteolytically released that have unpredictable effects, including for example a malignant transformation [28]. As seems the case, vipericidins have the potential to release hidden peptide sequences with the same or different activity than the parental molecule. Moreover, considering peptide diversity, synthesis and technical application, reduction of peptide size has obvious advantages [29]. In regard to svCRAMPs, Chen and co-workers [30] have prepared several peptides derived from BF-30 (Bf-CRAMP) and found that a 15-mer oligopeptide (*i.e.*, ^{157}VKRFKKFFRKLKKSV^{172}) retained the minimal helical structure necessary for potent antimicrobial activity. In another study, Zhang and collaborators [31] produced short synthetic analog peptides, which correspond to sequences internally embedded in *Ophiophagus hannah* cathelicidin (Oh-CRAMP, also Oh-CATH, 34 mer), and demonstrated that they display a distinct spectra of antimicrobial activity and hemolysis toward human erythrocytes compared to the original full sequence. Latour and colleagues [32] demonstrated that peptides derived from *Naja atra* cathelicidin, composed by the ATRA-motif, i.e, KR(F/A)KKFFKK(L/P)K, displayed high but variable potencies of antimicrobial activity with negligible toxicity to erythrocytes. Our study was centered on the C-terminal hypervariable acidic stretches of vipericidins and the first criptic amphiphatic nonapeptide peptide, KRFKKFFKK. The encrypted vipericidin nonapeptide sequences are practically identical in all svCRAMPs and appear repeatedly in tandem, with some conserved substitutions (Fig. 1). Incubation of zebrafish larvae with increasing concentrations of the rhodamine B-conjugated vipericidin-derived peptides (RhoB-ACPs and RhoB-EVPs) indicated that the peptides containing the amphiphatic nonapeptide KRFKKFFKK in their sequences (*i.e.*, RhoB-ACP1l and RhoB-ACP1b) and the cationic nonapeptide itself (named RhoB-EVP50) are extremely toxic. The calculated LD_{50} for these toxic peptides is in the micromolar range of concentration (16 μM, 13 μM and 6 μM, respectively) (Table 1). One possible explanation for the difference in the values of LD_{50} for the nonapeptide-containing ACPs in relation to RhoB-EVP50 might be the presence of the anionic piece just upstream of the cationic EVP50. It is believed that anionic prosequences in cathelicidins might help neutralize the net positive charge of the mature amphiphatic/cationic peptides and consequently abolish spatial-temporally the biological activity or decrease the cellular side effects in host cells [33]. Thus, we focused our attention in the encrypted nonapeptide and investigated the toxicity of unconjugated EVP50 using the same animal model. Unexpectedly, the EVP50 with unmodified amino-terminus was not toxic to zebrafish even at concentrations as high as 100 μM. Despite this fact and because peptides with covalently linked rhodamine B displayed changed and improved functionalities in certain cases [34], we monitored the distribution of the RhoB-EVP50 into the organs and tissues of zebrafish. With this goal in mind, *Tg*(*fli1:EGFP*) transgenic zebrafish were exposed to 10 μM RhoB-EVP50 for 24 h and visualized by fluorescence microscopy. As shown in Fig. 2 (A–H), RhoB-EVP50 heavily accumulates in the cardiovascular system (posterior and intersegment vasculature) of the zebrafish. It is interesting to note that RhoB-EVP50 easily penetrated and accumulated not only *in vivo* in the zebrafish organs (blood vessels and heart) but also *in vitro* in rat cardiomyocytes (H9c2 cardiomyoblasts) where intense red fluorescence was observable in whole cells and organelles (Fig. S1 and Video S1). Notably, free rhodamine B molecule was not taken up by cells and consequently was not distributed in the same tissues as the RhoB-conjugate EVP50. Indeed, it is known that free rhodamine B molecule has low bioavailability and low cell permeability in certain biological systems [35]. In concordance, with our data, but dissimilar biological effect, free rhodamine and unlabeled gelsolin-derived peptide lacked the ability to kill drug-resistant bacteria in an experimental study of bactericidal activities and the physicochemical properties of antibacterial peptides [34]. Consequently, the functionalization of the fluorescent dye molecule (*i.e.*, rhodamine B), experimentally observed here, was due to the EVP50 carrier core sequence. Our findings also support the work by El-Andaloussi and collaborators [36], which showed the cargo-dependence and the positional effect of cargo coupling on the toxicity of three different cell-penetrating peptides. Moreover, our data indicated that cells of cardiovascular system and tissues might be a target site for RhoB-EVP50 penetration; the cardiovascular system might also contain the preferential organs for peptide accumulation *in vivo* and the means by which zebrafish were poisoned.

In light of the facts that (1) RhoB-EVP50 accumulated *in vivo* in the cardiovascular system of zebrafish and in mammalian cardiomyocytes *in vitro* and that (2) elapid CRAMPs and analogs were cytotoxic against tumor cells [8,9], we decided to investigate the specific biological activity and toxicity of RhoB-EVP50 on selected cancer cell lines. Snake venom and spider venom have previously been reported to arrest breast cancer cell growth [37–39]. In our study, human breast cancer MCF-7 and MDA-MB-231 cells were used to test the anti-tumor activity of RhoB-EVP50. Fluorescent image analysis of MCF-7 incubated with 10 μM and 40 μM RhoB-EVP50 for 10 min showed that the Rhodamine B-conjugated nonapeptide rapidly internalized into the cell cytoplasm and distributed in the whole cells (Fig. 3). Within 60 min of incubation, the induced toxicity led to cell death and severely decreased the number of observable cells. Standard assays of cell viability and membrane

integrity showed that RhoB-EVP50 was cytotoxic to MCF-7 and MDA-MB-231 cells in a concentration-dependent manner (Fig. 4). Human lung carcinoma A549 cells were also induced to death in response to increasing concentration of RhoB-EVP50 (Fig. S2). Together, these properties of fast peptide uptake, intracellular accumulation and membrane disruption impart a toxic and cytotoxic capacity to the structurally modified encrypted nonapeptide to efficiently kill immortalized and malignant cells. As for *in vivo* model with zebrafish embryo, unconjugated EVP50 was inactive and unable of arresting cancer cells in culture (Fig. S2). Similar behavior was observed with nonmalignant cardiomyoblasts H9C2 cells, *i.e.*, the calculated IC_{50} values were practically identical as for cancer cells. Thus, the selectivity of the peptide was lower than expected and, therefore, remains to be improved, for example, by coupling to compounds and substances like drugs, lipids and other bioactive peptides, as well as nanoparticles [40]. Despite the lack of cell selectivity but prospective peptide modulation, these results imply that EVP50 is amenable to peptide design and engineering, with the aim of produce N-terminal conjugates with specific functionalities, seen that unconjugated EVP50 was harmless to eukaryotic cells. Coincidently, the short synthetic peptides derived from the basic ATRA-domain are not cytotoxic to eukaryotic cells [32] — the main structural difference between ATRA-domain and EVP50 nonapeptide is the presence of tripeptide K(L/P)K in the C-terminal.

Modulation of activity can also be seen with short synthetic analog peptides comprising sequences internally embedded in *O. hannah* cathelicidin. These short Oh-CRAMP derived peptides displayed a distinct spectrum of antimicrobial activity and hemolysis toward human erythrocytes. It was shown that the four N-terminal residues contribute to a hemolytic effect but not to the antimicrobial activity, whereas the ten C-terminal residues are necessary for both biological activities [31]. Other structural modification of svCRAMPs, which involve single amino acid substitution, *i.e.*, replacement of Lys for a Glu residue at position 16 (Cbf-K_{16}) in Bf-cathelicidin, improves the activity of the parental peptide against non-small lung cancer cells and antibiotic-resistant clinical isolates of *Escherichia coli* [8,41]. Consequently, the basic structural core of vipericidins, composed by EVP50 (KRFKKFFKK), can be further modulated and customized for the functionalization of probes (and therapeutic molecules), as well as for obtaining tailored biological activity. Most antimicrobial and anticancer (cytotoxic) peptides exert their effect by a direct single action (*e.g.*, physical disruption of cytoplasmic membrane) or a combination of synergic effects, such as formation of pores and cytoplasm leakage, translocation across lipid bilayers, and subsequent interactions with intracellular targets [42,43]. Cathelicidins are multifunctional antimicrobial peptides with immunomodulatory, tissue remodeling, angiogenic and anticancer activities. They can disrupt cell membranes and interact with DNA and thus are synergistically effective in killing cells, detain cell proliferation and recruit components of acquired immunity [43,44]. Thus, membrane interference/disruption and translocation followed by intracellular target interactions may separately or in combination play a role in cell cytotoxicity induced by cationic peptides [45–47]. These facts may serve as the basis to explain how RhoB-EVP50 exerts its action on cells. Measurements of intracellular calcium release after incubating MCF-7 cells in a micromolar concentration (30 μM) of peptide demonstrated that RhoB-EVP50 provoked an instantaneous and specific cellular calcium imbalance (increased extracellular calcium influx and intracellular calcium release) and consequent cytoplasm leakage (Fig. 5 and Video S2). Calcium homeostasis has been implicated in cell signaling for cell survival and death and is mediated by the interface between the mitochondria and the endoplasmic reticulum [48]. It is interesting to note that in some of fluorescent images from our experimental study, membrane budding was clearly observed (Video S2 and Fig. S3). Membrane budding and the formation of extracellular vesicles are associated with a plethora of intercellular messages, including pathological conditions of tumor progression, viral infection, immune responses, and microcystin-induced hepatoxicity and apoptosis [49,50]. As seen here, in addition to provoke membrane dysfunction, calcium imbalance and outward blebbing of the cell membrane appear to constitute early intracellular events in the cytotoxicity caused by RhoB-EVP50 uptake, followed by accumulation into the cytoplasm and sub-cellular structures of MCF-7 cells.

5. Conclusions

In the present work, we found that the hypervariable acidic moieties of the vipericidin carboxyl-termini exhibited reduced or were devoid of acute toxicity, whereas the lysine-rich encrypted amphiphatic nonapeptide conjugated to rhodamine B (RhoB-EVP50) displayed potent toxicity toward zebrafish and tumor cells in culture. In a transgenic zebrafish model, the encrypted nonapeptide was widely distributed and massively accumulated in the zebrafish cardiovascular system, which was lethal to the organism. Additionally, RhoB-EVP50 efficiently penetrated into rat ventricular cardiomyoblasts. Human breast cancer (MCF-7 and MDA-MB-231) cells were substantially sensitive to the biological effects of the vipericidin-encrypted peptide. In MCF-7 cells, RhoB-EVP50 caused observable calcium imbalance, membrane budding, membrane disruption, and cytoplasm leakage. The overall effect of RhoB-EVP50 was the induction of cell death over a short period of time, ranging from seconds to minutes. However, after peptide translocation, whether vesicle budding contributed to the spread of RhoB-EVP50 toxicity to tissue and organs, as observed in zebrafish larvae, remains to be further investigated. The fact that rhodamine B improves the efficiency of EVP50 in the translocation of dye-peptide conjugate into the cell and the EVP50 nonapeptide functionalizes the rhodamine B molecule, demonstrate that EVP50 arises as an alternative peptide sequence platform for application in the development of nanobiomaterials. Moreover, taking into account the findings reported here, a program of structure-activity modulation has been proposed using covalent linkage of molecules with distinct physicochemical properties to the basic core sequence of the EVP50 nonapeptide.

Supplementary data to this article can be found online at http://dx.doi.org/10.1016/j.bbagen.2015.02.013.

Transparency document

The Transparency document associated with this article can be found, in the online version.

Acknowledgments

Research at the University of Macao was supported by grants from the Science and Technology Development Fund (FDCT) of Macao — SAR 078/2011/A3 and 045/2007/A3 and the Research Committee of the University of Macau. Research at the Federal University of Ceará was supported by the Brazilian National Council for Scientific and Technological Development (CNPq), the Ministry of Science, Technology and Innovation (MCTI), the Program on Toxinology (Issue 2010), the Coordination for the Improvement of Higher Education Personnel (CAPES), and the Ministry of Education of the Federal Government of Brazil. We thank Ms. Christy Kou for her assistance with pre-screening activities of some peptides.

References

[1] C.B. Falcao, B.G. de La Torre, C. Pérez-Peinado, A.E. Barron, D. Andreu, G. Rádis-Baptista, Vipericidins: a novel family of cathelicidin-related peptides from the venom gland of South American pit vipers, Amino Acids 46 (2014) 2561–2571.
[2] Y. Wang, J. Hong, X. Liu, H. Yang, R. Liu, J. Wu, A. Wang, D. Lin, R. Lai, Snake cathelicidin from *Bungarus fasciatus* is a potent peptide antibiotics, PLoS One 3 (2008) e3217.
[3] H. Zhao, T.X. Gan, X.D. Liu, Y. Jin, W.H. Lee, J.H. Shen, Y. Zhang, Identification and characterization of novel reptile cathelicidins from elapid snakes, Peptides 29 (2008) 1685–1691.
[4] K. Konno, M. Hisada, R. Fontana, C.C.B. Lorenzi, H. Naoki, Y. Itagaki, A. Miwa, N. Kawai, Y. Nakata, T. Yasuhara, J. Ruggiero Neto, W.F. de Azevedo Jr., M.S. Palma, T.

Nakajima, Anoplin, a novel antimicrobial peptide from the venom of the solitary wasp *Anoplius samariensis*, Biochim. Biophys. Acta 1550 (2001) 70–80.
[5] M.P.D. Cabrera, B.M. de Souza, R. Fontana, K. Konno, M.S. Palma, W.F. de Azevedo Jr., J. Ruggiero Neto, Conformation and lytic activity of eumenine mastoparan: a new antimicrobial peptide from wasp venom, J. Pept. Res. 64 (2004) 95–103.
[6] Y. Wang, Z. Zhang, L. Chen, H. Guang, Z. Li, H. Yang, J. Li, D. You, H. Yu, R. Lai, Cathelicidin-BF, a snake cathelicidin-derived antimicrobial peptide, could be an excellent therapeutic agent for acne vulgaris, PLoS One 6 (2011) e22120.
[7] J. Wang, B. Li, Y. Li, J. Dou, Q. Hao, Y. Tian, H. Wang, C. Zhou, BF-30 effectively inhibits ciprofloxacin-resistant bacteria in vitro and in a rat model of vaginosis, Arch. Pharm. Res. 37 (2013) 927–936.
[8] H. Wang, M. Ke, Y. Tian, J. Wang, B. Li, Y. Wang, J. Dou, C. Zhou, BF-30 selectively inhibits melanoma cell proliferation via cytoplasmic membrane permeabilization and DNA-binding in vitro and in B16F10-bearing mice, Eur. J. Pharmacol. 707 (2013) 1–10.
[9] Y. Tian, H. Wang, B. Li, M. Ke, J. Wang, J. Dou, C. Zhou, The cathelicidin-BF Lys16 mutant Cbf-K16 selectively inhibits non-small cell lung cancer proliferation in vitro, Oncol. Rep. 30 (2013) 2502–2510.
[10] G. Rádis-Baptista, N. Oguiura, M.A. Hayashi, M.E. Camargo, K.F. Grego, E.B. Oliveira, T. Yamane, Nucleotide sequence of crotamine isoform precursors from a single South American rattlesnake (*Crotalus durissus terrificus*), Toxicon 37 (1999) 973–984.
[11] B.G. Fry, N. Vidal, J.A. Norman, F.J. Vonk, H. Scheib, S.F. Ramjan, S. Kuruppu, K. Fung, S.B. Hedges, M.K. Richardson, W.C. Hodgson, V. Ignjatovic, R. Summerhayes, E. Kochva, Early evolution of the venom system in lizards and snakes, Nature 439 (2006) 584–588.
[12] G. Anderluh, P. Macek, Cytolytic peptide and protein toxins from sea anemones (Anthozoa: Actiniaria), Toxicon 40 (2002) 111–124.
[13] R.S. Norton, Structures of sea anemone toxins, Toxicon 54 (2009) 1075–1088.
[14] M. Gmach, G. Kreil, The precursors of the bee venom constituents apamin and MCD peptide are encoded by two genes in tandem which share the same 3′-exon, J. Biol. Chem. 270 (1995) 12704–12708.
[15] V.S. Lee, W.C. Tu, T.R. Jinn, C.C. Peng, L.J. Lin, J.T. Tzen, Molecular cloning of the precursor polypeptide of mastoparan B and its putative processing enzyme, dipeptidyl peptidase IV, from the black-bellied hornet, *Vespa basalis*, Insect Mol. Biol. 16 (2007) 231–237.
[16] S. Luo, S. Christensen, D. Zhangsun, Y. Wu, Y. Hu, X. Zhu, S. Chhabra, R.S. Norton, J.M. McIntosh, A novel inhibitor of α9α10 nicotinic acetylcholine receptors from *Conus vexillum* delineates a new conotoxin superfamily, PLoS One 8 (2013) e54648.
[17] D.D. Yuan, Y.H. Han, C.G. Wang, C.W. Chi, From the identification of gene organization of alpha conotoxins to the cloning of novel toxins, Toxicon 49 (2007) 1135–1149.
[18] S.A. Kozlov, A.A. Vassilevski, A.V. Feofanov, A.Y. Surovoy, D.V. Karpunin, E.V. Grishin, Latarcins, antimicrobial and cytolytic peptides from the venom of the spider *Lachesana tarabaevi* (Zodariidae) that exemplify biomolecular diversity, J. Biol. Chem. 281 (2006) 20983–20992.
[19] D.J. Autelitano, A. Rajic, A.I. Smith, M.C. Berndt, L.L. Ilag, M. Vadas, The cryptome: a subset of the proteome, comprising cryptic peptides with distinct bioactivities, Drug Discov. Today 11 (2006) 306–314.
[20] Y. Xiao, Y. Cai, Y.R. Bommineni, S.C. Fernando, O. Prakash, S.E. Gilliland, G. Zhang, Identification and functional characterization of three chicken cathelicidins with potent antimicrobial activity, J. Biol. Chem. 281 (2006) 2858–2867.
[21] G. Hu, G.B. Mahady, S. Li, M.P. Hoi, Y.H. Wang, S.M. Lee, Polysaccharides from astragali radix restore chemical-induced blood vessel loss in zebrafish, Vasc. Cell 4 (2012) 2.
[22] Y.J. Oh, T.C. Gamble, D. Leonhardt, C.H. Chung, S.R. Brueck, C.F. Ivory, G.P. Lopez, D.N. Petsev, S.M. Han, Monitoring FET flow control and wall adsorption of charged fluorescent dye molecules in nanochannels integrated into a multiple internal reflection infrared waveguide, Lab Chip 8 (2008) 251–258.
[23] T. Uzzell, E.D. Stolzenberg, A.E. Shinnar, et al., Hagfish intestinal antimicrobial peptides are ancient cathelicidins, Peptides 24 (2003) 1655–1667.
[24] U.H.N. Durr, U.S. Sudheendra, A. Ramamoorthy, LL-37, the only human member of the cathelicidin family of antimicrobial peptides, Biochim. Biophys. Acta 1758 (2006) 1408–1425.
[25] L. Tomasinsig, M. Zanetti, The cathelicidins–structure, function and evolution, Curr. Protein Pept. Sci. 6 (2005) 23–34.
[26] F. Liu, G. Wets, A neural network method for prediction of proteolytic cleavage sites in neuropeptide precursors, Conf. Proc. IEEE Eng. Med. Biol. Soc. 3 (2005) 2805–2808.
[27] J.H. Wardman, L.D. Fricker, ProSAAS-Derived peptides are differentially processed and sorted in mouse brain and AtT-20 cells, PLoS One 9 (2014) e104232.
[28] F.T. Stevenson, J. Turck, R.M. Locksley, D.H. Lovett, The N-terminal propiece of interleukin 1 alpha is a transforming nuclear oncoprotein, Proc. Natl. Acad. Sci. U. S. A. 94 (1997) 508–513.
[29] C. Chen, J. Hu, P. Zeng, F. Pan, M. Yaseen, H. Xu, J.R. Lu, Molecular mechanisms of anticancer action and cell selectivity of short α-helical peptides, Biomaterials 35 (2014) 1552–1561.
[30] W. Chen, B. Yang, H. Zhou, L. Sun, J. Dou, H. Qian, W. Huang, Y. Mei, J. Han, Structure-activity relationships of a snake cathelicidin-related peptide, BF-15, Peptides 32 (2011) 2497–2503.
[31] Y. Zhang, H. Zhao, G.Y. Yu, X.D. Liu, J.H. Shen, W.H. Lee, Y. Zhang, Structure-function relationship of king cobra cathelicidin, Peptides 31 (2010) 1488–1493.
[32] F.A. de Latour, L.S. Amer, E.A. Papanstasiou, B.M. Bishop, M.L. van Hoek, Antimicrobial activity of the *Naja atra* cathelicidin and related small peptides, Biochem. Biophys. Res. Commun. 396 (4) (2010 Jun 11) 825–830.
[33] D. Michaelson, J. Rayner, M. Couto, T. Ganz, Cationic defensins arise from charge-neutralized propeptides: a mechanism for avoiding leukocyte autocytotoxicity? J. Leukoc. Biol. 51 (1992) 634–639.
[34] R. Bucki, J.J. Pastore, P. Randhawa, R. Vegners, D.J. Weiner, P.A. Janmey, Antibacterial activities of rhodamine B-conjugated gelsolin-derived peptides compared to those of the antimicrobial peptides cathelicidin LL37, magainin II, and melittin, Antimicrob. Agents Chemother. 48 (2004) (1526-1233).
[35] L.F. Mottram, S. Forbes, B.D. Ackley, B.R. Peterson, Hydrophobic analogues of rhodamine B and rhodamine 101: potent fluorescent probes of mitochondria in living *C. elegans*, Beilstein J. Org. Chem. 8 (2012) 2156–2165.
[36] S. El-Andaloussi, P. Järver, H.J. Johansson, U. Langel, Cargo-dependent cytotoxicity and delivery efficacy of cell-penetrating peptides: a comparative study, Biochem. J. 407 (2007) 285–292.
[37] M.K. Al-Sadoon, M.A. Abdel-Maksoud, D.M. Rabah, G. Badr, Induction of apoptosis and growth arrest in human breast carcinoma cells by a snake (*Walterinnesia aegyptia*) venom combined with silica nanoparticles: crosstalk between Bcl2 and caspase 3, Cell. Physiol. Biochem. 30 (2012) 653–665.
[38] K.L. Lin, J.C. Su, C.M. Chien, P.W. Chuang, L.S. Chang, S.R. Lin, Down-regulation of the JAK2/PI3K-mediated signaling activation is involved in Taiwan cobra cardiotoxin III-induced apoptosis of human breast MDA-MB-231 cancer cells, Toxicon 55 (2010) 1263–1273.
[39] L. Gao, S. Yu, Y. Wu, B. Shan, Effect of spider venom on cell apoptosis and necrosis rates in MCF-7 cells, DNA Cell Biol. 26 (2007) 485–489.
[40] H. Pan, Q. Zheng, S. Yang, X. Guo, Effects of functionalization of PLGA-[Asp-PEG]n copolymer surfaces with Arg-Gly-Asp peptides, hydroxyapatite nanoparticles, and BMP-2-derived peptides on cell behavior in vitro, J. Biomed. Mater. Res. A 102 (2014) 4526–4535.
[41] Q. Hao, H. Wang, J. Wang, J. Dou, M. Zhang, W. Zhou, C. Zhou, Effective antimicrobial activity of Cbf-K16 and Cbf-A7 A13 against NDM-1-carrying *Escherichia coli* by DNA binding after penetrating the cytoplasmic membrane in vitro, J. Pept. Sci. 19 (2013) 173–180.
[42] K.A. Brogden, Antimicrobial peptides: pore formers or metabolic inhibitors in bacteria? Nat. Rev. Microbiol. 3 (2005) 238–250.
[43] P. Nicolas, Multifunctional host defense peptides: intracellular-targeting antimicrobial peptides, FEBS J. 276 (2009) 6483–6496.
[44] J.H. Wong, X.J. Ye, T.B. Ng, Cathelicidins: peptides with antimicrobial, immunomodulatory, anti-inflammatory, angiogenic, anticancer and procancer activities, Curr. Protein Pept. Sci. 14 (6) (Sep. 2013) 504–514.
[45] R. Bucki, K. Leszczyńska, A. Namiot, W. Sokołowski, Cathelicidin LL-37: a multitask antimicrobial peptide, Arch. Immunol. Ther. Exp. 58 (2010) 15–25.
[46] N. Do, G. Weind, L. Grohmann, M. Salwiczek, B. Koksch, H.C. Korting, M. Schäfer-Korting, Cationic membrane-active peptides — anticancer and antifungal activity as well as penetration into human skin, Exp. Dermatol. 23 (2014) 326–331.
[47] M. Wenzel, A.I. Chiriac, A. Otto, D. Zweytick, C. May, C. Schumacher, R. Gust, H.B. Albada, M. Penkova, U. Krämer, R. Erdmann, N. Metzler-Nolte, S.K. Straus, E. Bremer, D. Becher, H. Brötz-Oesterhelt, H.G. Sahl, J.E. Bandow, Small cationic antimicrobial peptides delocalize peripheral membrane proteins, Proc. Natl. Acad. Sci. U. S. A. 111 (2014) E1409–E1418.
[48] D. Naon, L. Scorrano, At the right distance: ER-mitochondria juxtaposition in cell life and death, Biochim. Biophys. Acta 1843 (2014) 2184–2194.
[49] C. Krakstad, L. Herfindal, B.T. Gjertsen, R. Bøe, O.K. Vintermyr, K.E. Fladmark, S.O. Døskeland, CaM-kinaseII-dependent commitment to microcystin-induced apoptosis is coupled to cell budding, but not to shrinkage or chromatin hypercondensation, Cell Death Differ. 13 (2006) 1191–1202.
[50] S. EL Andaloussi, I. Mäger, X.O. Breakefield, M.J. Wood, Extracellular vesicles: biology and emerging therapeutic opportunities, Nat. Rev. Drug Discov. 12 (2013) 347–357.